Direct measurements of inverse magnetocaloric effects in metamagnetic shape-memory alloy NiCoMnIn

T. Kihara,[1,*] X. Xu,[2] W. Ito,[3] R. Kainuma,[2] and M. Tokunaga[1]
[1]*The Institute for Solid State Physics, The University of Tokyo, Kashiwa, Chiba 277-8581, Japan*
[2]*Department of Materials Science, Tohoku University, Sendai 980-8579, Japan*
[3]*Materials Science and Engineering, Sendai National College of Technology, Natori 981-1239, Japan*
(Received 2 December 2013; revised manuscript received 17 September 2014; published 2 December 2014)

To clarify the electronic, lattice, and magnetic contribution to the inverse magnetocaloric effect (IMCE) in the metamagnetic shape-memory alloy $Ni_{45}Co_5Mn_{50-x}In_x$, magnetization, magnetocaloric effect, and specific-heat measurements were carried out in a wide range of fields and temperatures. The IMCEs of $Ni_{45}Co_5Mn_{36.7}In_{13.3}$ were directly measured as adiabatic temperature changes in pulsed fields of up to 15 T. A maximum temperature decrease of −12.8 K was observed. The low-temperature specific heats in both the austenitic and the martensitic phases of $Ni_{45}Co_5Mn_{36.5}In_{13.5}$ were measured by using steady fields. Through analyses of the data, the entropy changes in charge (1.2 J/kg K), spin (−29 J/kg K), and lattice (51 J/kg K) sectors were individually evaluated. The result demonstrates the dominant role of the lattice sector in inverse MCEs in this material.

DOI: 10.1103/PhysRevB.90.214409 PACS number(s): 75.30.Sg, 81.30.Kf

I. INTRODUCTION

The recent discovery of giant magnetocaloric effects (GMCEs) at around room temperatures has triggered the development of a magnetic refrigerator that operates at ambient temperatures [1,2]. The GMCE appears as a result of the simultaneous entropy changes in different degrees of freedom (spin, lattice, orbital, etc.). Therefore, the total entropy change can exceed the magnetic entropy change caused by the forced spin alignment. Owing to the strong coupling between the spin and the lattice subsystems, materials showing GMCEs usually undergo first-order magnetostructural transitions [1–11].

Ni-Mn-Z (Z = In, Sn, Sb) metamagnetic shape-memory alloys have attracted considerable attention as candidates for novel rare-earth free magnetic refrigerants [1,12–14]. These materials undergo martensitic transformations (MTs) from a high-temperature ferromagnetic austenite phase (A phase: cubic, $L2_1$) to a low-temperature paramagnetic martensite phase (M phase: monoclinic) at around room temperature. The application of a magnetic field to the M phase under isothermal conditions realizes magnetic-field-induced martensitic transformation (MFIMT). Thermodynamic analyses of the MFIMT reveal a great increase in entropy at the transition, contrary to the intuitive expectation of reduction in spin entropy owing to forced spin alignment [12,13]. This unconventional and unexpected phenomenon is called the inverse magnetocaloric effect (IMCE) [12–15]. The IMCE indicates positive changes in entropy through the MFIMT that dominates over the negative changes caused by spin ordering. For this class of materials, the total entropy change at the MFIMT (ΔS_{tot}) can be decomposed as $\Delta S_{tot} = \Delta S_{ele} + \Delta S_{lat} + \Delta S_{mag}$, where ΔS_{ele}, ΔS_{lat}, and ΔS_{mag} respectively denote the electric, lattice, and magnetic contribution of the entropy change.

Any of ΔS_{ele}, ΔS_{lat}, and ΔS_{mag} can contribute to the IMCE. Since the MTs in Ni-Mn-based Heusler alloys are attributed to the band Jahn-Teller effect [11,16], we can expect a significant change in the density of states (DOS) at the Fermi level and in turn, in the Sommerfeld coefficient of the electronic specific heat. This idea is consistent with the several experimental studies that reported increases in the electric conductivity through the MFIMT [17–19]. Vasiliev *et al.* measured the specific heat of Ni-Co-Mn-In alloy in the paramagnetic M phase [17]. They compared its Sommerfeld coefficient with those reported for the ferromagnetic A phase of the related materials [20,21] and claimed that the electronic specific heats in the two phases were significantly different [17]. However, it is unclear whether such a considerable change emerges in the same compound, because the physical properties of this class of materials are highly sensitive to the composition.

Second, the discovery of the metamagnetic shape-memory effect [13] and the magnetovolume effect [22] indicates the importance of the entropy change in the lattice system. Liu *et al*. claimed that this contribution can play a dominant role in the IMCE of Ni-Co-Mn-In; however, they did not provide a quantitative evaluation of the lattice contribution to the IMCE [14].

Third, the magnetic contribution to the entropy should be taken into account. As mentioned previously, the transition from the paramagnetic to the ferromagnetic phase reduces spin entropy. Furthermore, the MFIMT in this material is accompanied by an increase of DOS at Fermi energy, which can elongate the magnetic moment. This effect contributes to the positive entropy change. A positive entropy change caused by an increase in magnetic moment has already been reported for a valence transition material [23]. Competition between these components can result in either positive or negative MCE.

Numerous studies have attempted to gain a comprehensive understanding of the IMCE in these Heusler alloys through indirect methods such as magnetization and/or specific heat near the transition temperature [24–26]. However, those thermodynamic measurements under limited conditions can only reveal the change in total entropy. In addition, direct measurement of the MCE is crucial for an in-depth understanding of this phenomenon. Although previous studies

*t_kihara@imr.tohoku.ac.jp

investigated the adiabatic temperature change in these Heusler alloys under magnetic fields of up to 1.9 T [14,27], this field is insufficient to complete the MFIMT. Therefore, the hysteretic nature that is inevitable in these first-order transitions hinders a quantitative interpretation of the MCE results. In the present study, we investigated the IMCE of $Ni_{45}Co_5Mn_{50-x}In_x$ alloys in a wide range of temperatures and magnetic fields using newly developed direct experimental techniques [28–30]. Based on these results, we discuss the electronic, structural, and magnetic contribution to entropy change individually.

II. EXPERIMENTS

Polycrystalline samples of $Ni_{45}Co_5Mn_{50-x}In_x$ ($x = 13.3$, 13.5 at.%) were used for the experiments. These samples were obtained by annealing the ingots, which were prepared by the induction melting method, at 900°C for 24 h under argon atmosphere. MCE measurements in pulsed high magnetic fields were performed for $Ni_{45}Co_5Mn_{36.7}In_{13.3}$. To measure the sample temperature that changes instantaneously in the pulsed field, a patterned Au resistive thermometer (thickness: 100 nm) was deposited on a sapphire disk (thickness: 5 μm). Then, the sapphire disk with the thermometer was placed on top of the sample with a small amount of Apiezon® N grease. The pulsed fields are generated by the 55-T magnet (duration: 36 ms) at the Institute for Solid State Physics, the University of Tokyo. The isothermal magnetization under pulsed fields is detected using a coaxial-type pick-up coil located at the center of the pulse magnet. To realize isothermal measurements under pulsed fields, the sample was thermally contacted to the large quartz block with silicone grease. The structural change of the sample surface through a MFIMT in $Ni_{45}Co_5Mn_{36.5}In_{13.5}$ was observed using the high-speed imaging system for a pulsed field of up to 35 T [28]. The sample surface was polished to be optically flat at room temperature.

The heat-capacity measurements in zero and steady fields are performed using a differential scanning calorimeter (DSC, 204F1 Phenix®, NETZSCH) and a relaxation-type calorimeter (Physical Property Measurement System, QuantumDesign).

III. RESULTS AND DISCUSSION

We show the MCEs of $Ni_{45}Co_5Mn_{36.7}In_{13.3}$ directly measured in pulsed high magnetic fields (Fig. 1). The sample is in the ferromagnetic A phase at 310 K. Applying a magnetic field at this temperature causes monotonic heating of the sample, which can be attributed to the conventional MCE caused by the forced spin alignment by the applied fields. The present result at 310 K shows a reversible trace between field-increasing and -decreasing processes, as expected in the conventional MCEs, indicating the experimental validity, i.e., negligible heat exchange to the surroundings and fast response in the thermometer, in the present measurements [30]. The results at 250–300 K are the MCEs when the magnetic fields are applied in the M phase. As the field increases, the sample temperature steeply decreases (IMCE) at the MFIMT, followed by a positive slope in the high-field A phase. In the successive field-decreasing process, the sample heats up to approximately

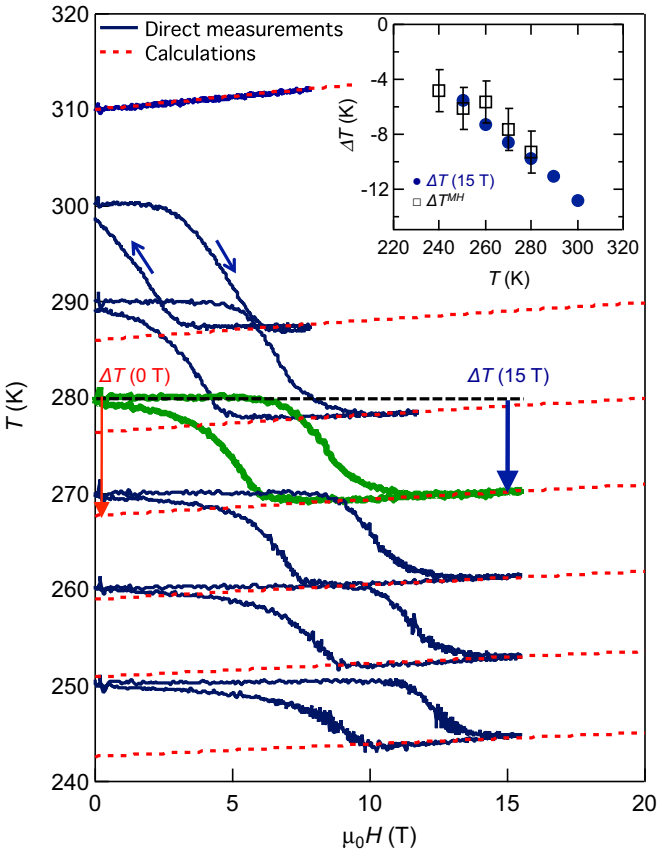

FIG. 1. (Color online) Temperatures of $Ni_{45}Co_5Mn_{36.7}In_{13.3}$ sample during the adiabatic magnetization processes in pulsed magnetic fields. Inset: directly measured adiabatic temperature change ΔT (15 T) and that calculated from isothermal magnetization curves ΔT^{MH} shown as a function of temperature.

10 K at the MFIMT. The coincidence of the initial and final temperatures at the zero field indicates that the heating caused by hysteresis loss is negligible in comparison to the MCEs [30]. The inset of Fig. 1 shows the temperature change caused by an external field of 15 T, which is defined as ΔT (15 T) and indicated by the thick arrow in Fig. 1 as a function of the initial temperature. ΔT (15 T) increases linearly as the initial temperature decreases from the transition temperature at zero field. This ΔT (15 T) contains conventional MCE by forced spin alignment in the A phase. To evaluate the entropy difference in the two phases at zero field, we subtract this component by extrapolating the high-field T-H traces to zero field and evaluating ΔT (0T) as indicated by the thin arrow in Fig. 1. The estimated ΔT (0 T) $= -13.8$ K at 300 K corresponds to the isothermal entropy change $\Delta S_{\rm tot} \simeq -C\Delta T/T =$ 22 J/kg K. Here, we used specific heat $C = 485$ J/kg K [see Fig. 2(a)].

To check the validity of this value, we evaluated the $\Delta S_{\rm tot}$ by the specific-heat measurements at zero field for $Ni_{45}Co_5Mn_{36.7}In_{13.3}$ (In13.3) and $Ni_{45}Co_5Mn_{36.5}In_{13.5}$ (In13.5), respectively. Figure 2(a) shows the results measured on the warming process. The peaks at 317 K for In13.3 and at 312 K for In13.5 are due to the latent heat released at MT. The shoulders at 387 K for In13.3 and at 383 K for In13.5 correspond to the Curie temperature (T_C) in the A phase. The

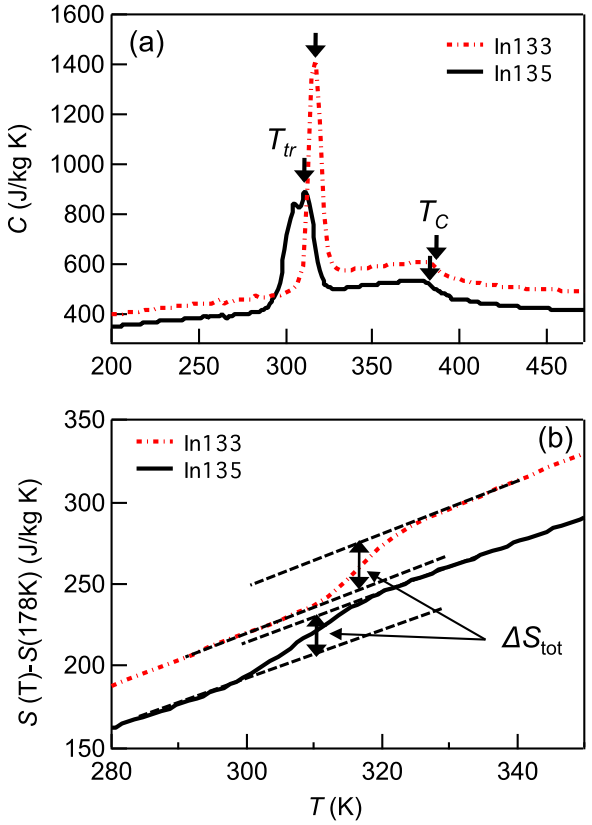

FIG. 2. (Color online) (a) Specific heats and (b) entropy of $Ni_{45}Co_5Mn_{36.7}In_{13.3}$ (red dash-dotted curve) and $Ni_{45}Co_5Mn_{36.5}In_{13.5}$ (black solid curve) measured using a DSC.

temperature dependencies of the entropy were calculated from those data as shown in Fig. 2(b). The ΔS_{tot} indicated by arrows in Fig. 2(b) is estimated as 25 J/kg K (1.6 J/mol K) for In13.3 and 26 J/kg K (1.7 J/mol K) for In13.5, which are in reasonable agreement with that estimated from the MCE measurement described above. The ΔS_{tot} includes the electron, lattice, and magnetic contributions. Thus, we next discuss the method to estimate these contributions individually.

To evaluate the MCEs, we need to know the entropy as a function of the magnetic field not only at around the MFIMT, but also in the M and A phases. Thus we performed magnetization measurements in pulsed magnetic fields at various temperatures to evaluate later the magnetic contribution to the entropy in a wide range of the temperatures and the fields. Figures 3(a) and 3(b) show the M-H curves of In13.3 and In13.5, respectively. In both compositions, magnetic fields of 25 T can complete the MFIMT in the entire temperature range. The saturated magnetization in the ferromagnetic A phase is estimated as $M_s = 1.68\mu_B$/f.u. for In13.3 and $M_s = 1.76\mu_B$/f.u. for In13.5 at 4.2 K. Here, $Ni_{0.45}Co_{0.05}Mn_{0.50-x}In_x$ is defined as one formula unit (f.u.). For In13.3, the MCEs are calculated from the M-H curves using

$$\Delta T = -\int_0^H \frac{T}{C_H}\left(\frac{\partial M}{\partial T}\right)_H dH'. \quad (1)$$

The results are indicated by open squares in the inset of Fig. 1. The calculated ΔT^{MH}'s are in reasonable agreement with the

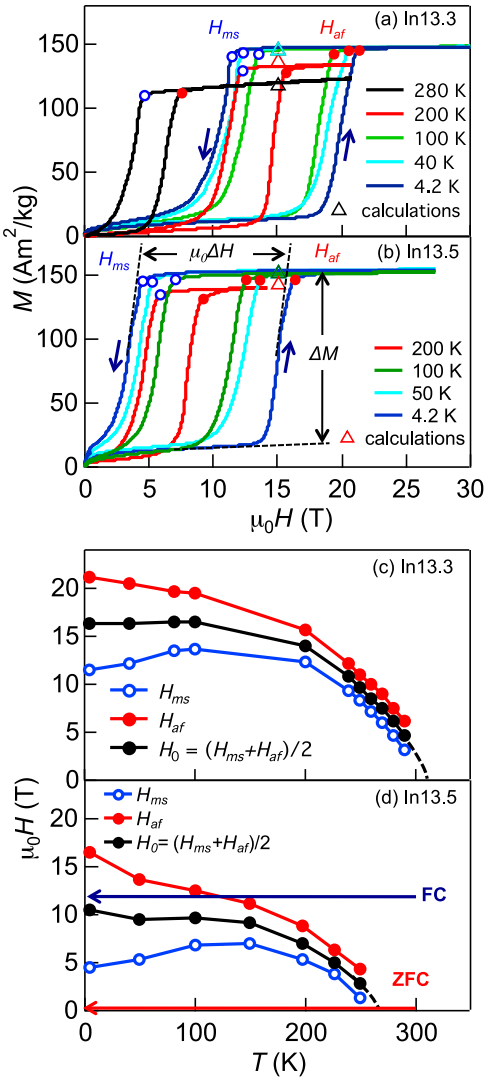

FIG. 3. (Color online) M-H curves measured in the pulsed magnetic fields: (a) $Ni_{45}Co_5Mn_{36.7}In_{13.3}$ (In13.3), (b) $Ni_{45}Co_5Mn_{36.5}In_{13.5}$ (In13.5). Magnetic phase diagram: (c) In13.3, (d) In13.5.

directly measured ones. The energy dissipation is estimated as $\mu_0 \oint HdM \simeq 307$ J/kg from the area of the hysteresis in the M-H curve at 280 K. Here, μ_0 is the space permeability. Under adiabatic conditions, the possible heating caused by this hysteresis loss is estimated to be 0.67 K, which is less than 7% of the IMCE at the same temperature. Therefore, most of the observed temperature changes in Fig. 1 are attributed to entropy changes. By defining their MT fields by open and solid circles in Figs. 3(a) and 3(b), the magnetic phase diagrams for In13.3 and In13.5 are obtained as shown in Figs. 3(c) and 3(d), respectively. ΔS_{tot} through MFIMT can be estimated from the Clausius-Clapeyron equation: $\mu_0 dH_0/dT = -\Delta S_{tot}/\Delta M$, where $H_0 \equiv (H_{ms} + H_{af})/2$. ΔS_{tot} at the transition temperature in the zero field is estimated to be 26 J/kg K (In13.3) and 23 J/kg K (In13.5). These results are in good agreement with the values obtained from the specific-heat measurements [see Fig. 2(b) and Ref. [31]].

Before calculating the magnetic entropy from the M-H curves, we should clarify whether finite slopes of the M-H

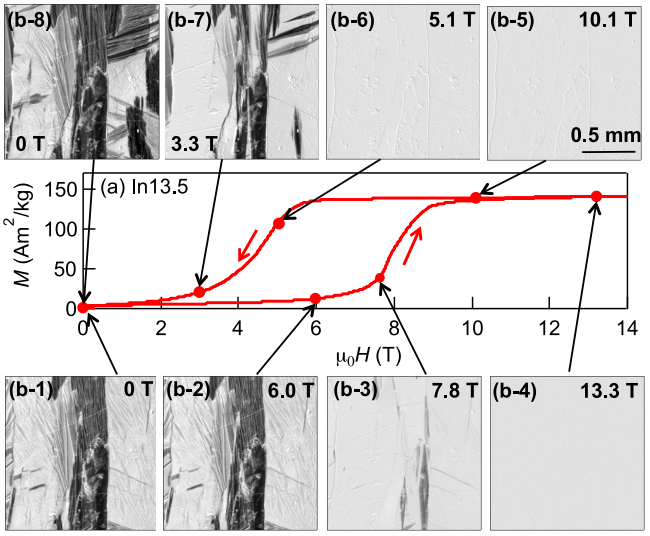

FIG. 4. (Color online) (a) M-H curve and (b) micrographs of the sample surface for $Ni_{45}Co_5Mn_{36.5}In_{13.5}$ at 200 K. The images at the highest field were subtracted from each image to obscure scratches and contaminants.

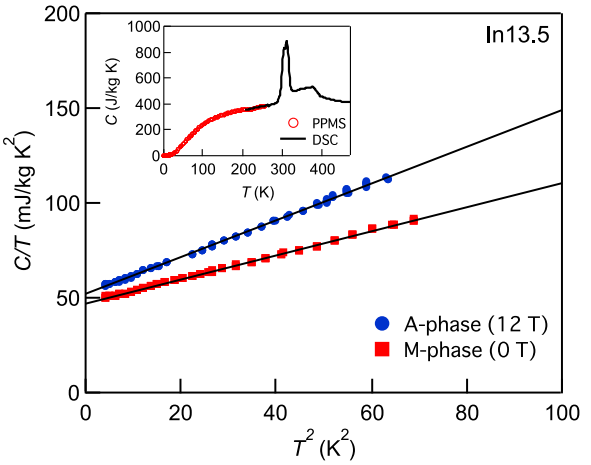

FIG. 5. (Color online) Specific heat C of $Ni_{45}Co_5Mn_{36.5}In_{13.5}$ (In13.5) plotted as C/T vs T^2. The data of A phase (12 T) were measured after field cooling at 12 T. Inset: C vs T of In13.5 at zero field in the temperature range 2–471 K.

curves observed in the low-field region involve local MFIMT. Such local transition can be detected using our high-speed microscope system combined with a miniature pulse magnet [28]. Figures 4(a) and 4(b) show the M-H curve and micrographs of the sample surfaces for In13.5 in various fields at 200 K. The sample surface, which is polished in the A phase, showed buckling upon cooling into the M phase, as shown in Fig. 4(b-1). Here, the image at the maximum field (13.4 T) is subtracted from others to obscure extrinsic features such as scratches or contaminants. When the magnetic field is applied normal to the sample surface, the surface morphology started changing at around 6 T, and became stable above H_{af} [Figs. 4(b-2)–4(b-4)]. In the successive field-decreasing process [Figs. 4(b-5)–4(b-8)], the M phase appears below 5.1 T. The entire process of the MFIMT is shown as movies for differential and pristine images in the Supplemental Information (1 and 2) [32]. Xu *et al.* [33] showed that the contrast in the micrograph is a good indicator for the volume fraction of the M phase. Therefore, the MFIMT occurs only in the field region where the magnetization changes steeply. In other words, we can safely analyze the data assuming a single M or A phase in the other field region.

Then, we discuss MCEs in the field region apart from the MFIMT, where changes in the spin entropy in a given phase mainly contribute to this effect. Here, we consider the following simple molecular field model:

$$M = Ng\mu_B J B_J\left(\frac{g\mu_B J\mu_0(H-\lambda M)}{k_B T}\right), \qquad (2)$$

Here, B_J is the Brillouin function. $N \simeq 6.02\times10^{23}$ mol^{-1} is Avogadro's number. We set the g factor as $g = 2$. The coefficient λ represents the magnetic interaction and is defined as $\lambda = 3k_B T_\Theta/Ng^2\mu_B^2 J(J+1)$ by the Weiss temperature T_Θ. Substituting $gJ = 1.68\mu_B$/f.u. (estimated from the M-H curves) and $T_\Theta \simeq T_C = 387$ K [determined from Fig. 2(a)], the magnetization of the A phase can be calculated without any free parameters. The results at 15 T are plotted as open triangles in Figs. 3(a) and 3(b). Despite this crude approximation, the calculated magnetizations are in reasonable agreement with the experimental ones. The MCE as a function of magnetic field is obtained using Eq. (1) from the calculated M-H curve. The results indicated by the dashed lines in Fig. 1 are in reasonable agreement with the directly measured data. This agreement indicates that the temperature and magnetic field dependence of the magnetic entropy in the A phase can be calculated by this model. On the other hand, the MCE in the M phase is so small that the magnetic entropy in the M phase can hardly be calculated by this model.

Next, we performed specific-heat measurements at low temperatures to evaluate the electronic and lattice contributions to the entropy. As shown in Fig. 3(d), In13.5 remains in the A phase even at low temperatures through field cooling (FC) above 8 T. Thus, we measured the specific heat at low temperatures in the A phase and M phase for the same sample. The results are plotted as C/T against T^2 in Fig. 5. The data of the A phase are measured at a steady field of 12 T to minimize the magnetic component in C. The specific heats in both phases can be fitted by the sum of the linear Sommerfeld term γT and the cubic term of the Debye model βT^3 below 8 K, as indicated by the solid lines in Fig. 5. The Sommerfeld coefficient γ in the A phase [$\gamma = 52$ mJ/kg K^2 (3.4 mJ/mol K^2)] exceeds that of the M phase [$\gamma = 48$ mJ/kg K^2 (3.1 mJ/mol K^2)] by only 4 mJ/kg K^2. This value corresponds to the difference of entropy $\Delta S_{ele} = 1.2$ J/kg K at 300 K. Therefore, the electronic contribution to the IMCE is negligibly small.

In contrast, the Debye temperature Θ_D shows a remarkable difference of 47 K between the two phases [$\Theta_D = 314$ K (A phase) and 361 K (M phase)]. By using the simple Debye model, the difference of the lattice entropy ΔS_{lat} is calculated as $\Delta S_{lat} = 51$ J/kg K at 300 K. This value is approximately twice as large as the ΔS_{tot} values obtained from the phase diagram. Although the Debye model is a rough approximation, we can claim that the lattice contribution plays the dominant

role in the IMCE. We estimate the remaining entropy of the spin system by taking these results into account.

By substituting the estimated electronic and lattice entropies into $\Delta S_{tot} = \Delta S_{ele} + \Delta S_{lat} + \Delta S_{mag}$, the entropy of the spin system is calculated as $\Delta S_{mag} \simeq -29$ J/kg K (1.9 J/mol K) at 300 K. As mentioned previously, we can estimate the entropy of the spin system in the A phase S^{A}_{mag} using a simple model, which becomes 79 J/kg K (5.1 J/mol K) at 300 K for the In13.5 sample with $T^{A}_{C} = 383$ K and $J_A = 0.88$. Thus, the entropy of the spin system in the M phase is evaluated to be $S^{M}_{mag} = 108$ J/kg K (7.0 J/mol K). Since the MCEs in the M phase are negligibly small as seen in Fig. 1, we assume a random arrangement of spins in the M phase at least above 250 K. From the relation of $S^{M}_{mag} = R \ln(2J_M + 1) = 7.0$ J/mol K (R is the gas constant), we can estimate the magnetic moment of the M phase $gJ_M = 1.32\mu_B$/f.u. which is smaller than that of the A phase by 25%. Therefore, the magnetic entropy involves the contributions not only due to spin ordering but also due to change in the magnetic moment. If we assume the paramagnetic A phase, the magnetic entropy change due to the difference of magnetic moments is estimated as 22 J/kg K (1.4 J/mol K), which is comparable to ΔS_{tot}. In the magnetization process, the increase of magnetic moment at the MFIMT (from the M phase to the A phase) contributes to the positive entropy change. This effect, therefore, is competing with the negative entropy change due to the spin ordering. Totally, the magnetic system contributes to the negative entropy change at the MFIMT.

Next, we discuss the temperature dependence of the entropy difference between the M and the A phase. The temperature dependencies of S_{ele}, S_{lat}, and S^{A}_{mag} were calculated by the models described above. At present, we have no proper method to evaluate temperature dependence of the S^{M}_{mag}. As the specific heat of the M phase measured in a wide temperature range (inset of Fig. 5) does not show any feature for the occurrence of the magnetic order, we first assume random spin arrangement, i.e., no considerable change in the S^{M}_{mag} down to low temperatures. The calculated entropy difference in each sector is indicated in the inset of Fig. 6 by solid lines. Here, the horizontal axis is set to the difference between the MT temperature in zero or finite fields (T_{tr}) and Curie temperature (T_C) in the A phase. The calculated ΔS_{tot} coincides with the experimental results for $Ni_{50-y}Co_yMn_{50-x}In_x$ measured at various x and y values in the temperature range $T_C - T_{tr} \leqslant 100$ K [19,34]. For $T_{tr} > T_C$, the system undergoes a transition from the paramagnetic M phase to the paramagnetic A phase (shadowed area in Fig. 6), and therefore, the contribution of the spin alignment can be neglected. In this case, ΔS_{tot} is determined by the lattice entropy and the increase in the magnetic moment, which both show little temperature dependence. This result explains the reported large entropy changes for the materials with $T_{tr} > T_C$ [34]. For $T_{tr} < T_C$, ΔS_{tot} decreases with increasing $T_C - T_{tr}$ because the contribution of the spin alignment (negative entropy change) increases as T_{tr} deviates from T_C. Preceding studies on the developments of GMCE at MFIMT focus on the increase in T_C of materials to realize large ΔM at low fields. Our present result clarifies the negative aspect of higher T_C, which diminishes a significant fraction of the entropy available for MCEs. For large magnetic refrigerators, this aspect will be a deeper problem.

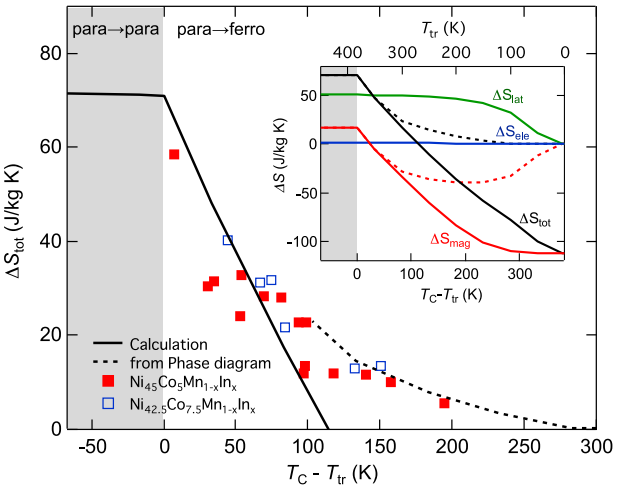

FIG. 6. (Color online) Entropy change through a martensitic transformation ΔS_{tot} vs $T_C - T_{tr}$. T_C and T_{tr} are the Curie point of the A phase and the martensitic transformation temperature, respectively. The solid line indicates the calculated result for In13.5 (Inset: $T_C - T_{tr}$ dependencies of ΔS_{ele}, ΔS_{lat}, ΔS_{mag}, and ΔS_{tot} in a wide range of temperatures). The dashed line indicates the estimation from the magnetic phase diagram shown in Fig. 3(d) using the Clausius-Clapeyron equation. The symbols are experimentally obtained data from the magnetization or heat-capacity measurements [19,34].

As $T_C - T_{tr}$ increases above 100 K, the calculated ΔS_{tot} no longer reproduces the experimental results. The dashed line in Fig. 6 represents the experimentally determined ΔS_{tot} from the analyses of the M-H curves and the phase diagrams in Fig. 3 using the Clausius-Clapeyron equation: $\mu_0 dH_0/dT = -\Delta S_{tot}/\Delta M$. This discrepancy can be ascribed to our improper assumption of the constant S^{M}_{mag}, which has to approach zero as the temperature decreases. In other words, the observed deviation represents the released magnetic entropy in the M phase. As shown in the inset of Fig. 5, there is no anomaly in the temperature dependence of the specific heat for the M phase (below 300 K); therefore, long-range ordering of the spin system does not occur. Further detailed experiments focusing on the magnetism in the M phase are highly desirable to clarify the origin of the reduction in S^{M}_{mag}.

IV. CONCLUSION

The inverse magnetocaloric effect (IMCE) of $Ni_{45}Co_5Mn_{36.7}In_{13.3}$ was directly measured under the pulsed high magnetic fields. Furthermore, the individual entropy changes in charge, spin, and lattice sector were evaluated by the combination of MCE and specific-heat measurements. We summarize the origins of the IMCE as follows. The change in the lattice entropy plays the dominant role in the IMCE of NiCoMnIn. The electronic contribution to the IMCE is negligibly small. The magnetic entropy involves two types of contributions that compete with each

other: increase in magnetic moment (positive entropy change) and spin ordering (negative entropy change). This magnetic contribution determines the composition dependence of the total entropy changes at the martensitic transformation temperature and field in $Ni_{1-y}Co_yMn_{1-x}In_x$.

ACKNOWLEDGMENT

This work was partly supported by the Ministry of Education, Culture, Sports, Science and Technology, Japan, through a Grant-in-Aid for Scientific Research (B) (Grant No. 23340096).

[1] E. Brück, J. Phys. D **38**, R381 (2005).
[2] V. K. Pecharsky and K. A. Gschneidner, Jr., Phys. Rev. Lett. **78**, 4494 (1997).
[3] W. Choe, V. K. Pecharsky, A. O. Pecharsky, K. A. Gschneidner, Jr., V. G. Young, Jr., and G. J. Miller, Phys. Rev. Lett. **84**, 4617 (2000).
[4] L. Morellon, J. Stankiewicz, B. Garcia-Landa, P. A. Algarabel, and M. R. Ibarra, Appl. Phys. Lett. **73**, 3462 (1998).
[5] L. Morellon, P. A. Algarabel, M. R. Ibarra, J. Blasco, B. Garcia-Landa, Z. Arnold, and F. Albertini, Phys. Rev. B **58**, R14721 (1998).
[6] L. Morellon, Z. Arnold, C. Magen, C. Ritter, O. Prokhnenko, Y. Skorokhod, P. A. Algarabel, M. R. Ibarra, and J. Kamarad, Phys. Rev. Lett. **93**, 137201 (2004).
[7] O. Tegus, E. Brück, K. H. J. Buschow, and F. R. de Boer, Nature (London) **415**, 150 (2002)
[8] S. Fujieda, A. Fujita, and K. Fukamichi, Appl. Phys. Lett. **81**, 1276 (2002).
[9] F. X. Hu, B. G. Shen, J. R. Sun, A. B. Pakhomov, C. Y. Wong, X. X. Zhang, S. Y. Zhang, G. J. Wang, and Z. H. Cheng, IEEE Trans. Magn. **37**, 2328 (2001).
[10] H. Wada and Y. Tanabe, Appl. Phys. Lett. **79**, 3302 (2001).
[11] S. Fujii, S. Ishida, and S. Asano, J. Phys. Soc. Jpn. **58**, 3657 (1989).
[12] T. Krenke, E. Duman, M. Acet, E. F. Wassermann, X. Moya, L. Mañosa, and A. Planes, Nat. Mater. **4**, 450 (2005).
[13] R. Kainuma, Y. Imano, W. Ito, Y. Sutou, H. Morito, S. Okamoto, O. Kitakami, K. Oikawa, A. Fujita, T. Kanomata, and K. Ishida, Nature (London) **439**, 957 (2006).
[14] J. Liu, T. Cottschall, K. P. Skokov, J. D. Moore, and O. Gutfleisch, Nat. Mater. **11**, 620 (2012).
[15] A. Planes, L. Mañosa, and M. Acet, J. Phys.: Condens. Matter **21**, 233201 (2009).
[16] M. Ye, A. Kimura, Y. Miura, M. Shirai, Y. T. Cui, K. Shimada, H. Namatame, M. Taniguchi, S. Ueda, K. Kobayashi, R. Kainuma, T. Shishido, K. Fukushima, and T. Kanomata, Phys. Rev. Lett. **104**, 176401 (2010).
[17] A. N. Vasiiev, O. Heczko, O. S. Volkova, T. N. Vasilchikova, T. N. Voloshok, K. V. Klimov, W. Ito, R. Kainuma, K. Ishida, K. Oikawa, and S. Fähler, J. Phys. D **43**, 055004 (2010).
[18] A. K. Pathak, B. R. Gautam, I. Dudenko, M. Khan, and S. Stadler, J. Appl. Phys. **103**, 07F315 (2008).
[19] S. Kustov, M. L. Corró, J. Pons, and E. Cesari, Appl. Phys. Lett. **94**, 191901 (2009).
[20] O. Heczko, S. Fähler, T. M. Vasilchikova, T. N. Voloshok, K. V. Klimov, Y. I. Chumlyakov, and A. N. Vasiiev, Phys. Rev. B **77**, 174402 (2008).
[21] M. Kreissl, K-U. Neumann, T. Stephens, and K. R. A. Ziebeck, J. Phys.: Condens. Matter **15**, 3831 (2003).
[22] Z. Li, C. Jing, H. L. Zhang, D. H. Yu, L. Chen, B. J. Kang, S. X. Cao, and J. C. Zhang, J. Appl. Phys. **108**, 113908 (2010).
[23] H. Wada, H. Gomi, A. Mitsuda, and M. Shiga, Solid State Commun. **117**, 703 (2001).
[24] F. Guillou, P. Courtois, L. Porcar, P. Plaindoux, D. Bourgault, and V. Hardy, J. Phys. D **45**, 255001 (2012).
[25] V. Recarte, J. I. Pérez-Landazábal, S. Kustov, and E. Cesari, J. Appl. Phys. **107**, 053501 (2010).
[26] V. A. Chernenko, J. M. Barandiarán, J. R. Fernández, D. P. Rojas, J. Gutiérrez, P. Lázpita, and I. Orue, J. Magn. Magn. Mater. **324**, 3519 (2012).
[27] V. V. Khovaylo, K. P. Skokov, O. Gutfleisch, H. Miki, R. Kainuma, and T. Kanomata, Appl. Phys. Lett. **97**, 052503 (2010).
[28] I. Katakura, M. Tokunaga, A. Matsuo, K. Kawaguchi, K. Kindo, M. Hitomi, D. Akahoshi, and H. Kuwahara, Rev. Sci. Instrum. **81**, 043701 (2010).
[29] T. Kihara, I. Katakura, M. Tokunaga, A. Matsuo, K. Kawaguchi, A. Kondo, K. Kindo, W. Ito, X. Xu, and R. Kainuma, J. Alloy. Compd. **577**, S722 (2013).
[30] T. Kihara, Y. Kohama, Y. Hashimoto, S. Katsumoto, and M. Tokunaga, Rev. Sci. Instrum. **84**, 074901 (2013).
[31] X. Xu, W. Ito, R. Y. Umetsu, R. Kainuma, and K. Ishida, Appl. Phys. Lett. **95**, 181905 (2009).
[32] See Supplemental Material at http://link.aps.org/supplemental/10.1103/PhysRevB.90.214409 for the entire process of the MFIMT as movies. (1) The image at the maximum field is subtracted from others, to obscure extrinsic features such as scratches and contaminants. (2) The pristine movie.
[33] X. Xu, W. Ito, I. Katakura, M. Tokunaga, and R. Kainuma, Scr. Mater. **65**, 946 (2011).
[34] W. Ito, Y. Imano, R. Kainuma, Y. Sutou, K. Oikawa, and K. Ishida, Metall. Mater. Trans. A **38**, 759 (2007).